

NJC

Accepted Manuscript



This is an *Accepted Manuscript*, which has been through the Royal Society of Chemistry peer review process and has been accepted for publication.

Accepted Manuscripts are published online shortly after acceptance, before technical editing, formatting and proof reading. Using this free service, authors can make their results available to the community, in citable form, before we publish the edited article. We will replace this *Accepted Manuscript* with the edited and formatted *Advance Article* as soon as it is available.

You can find more information about *Accepted Manuscripts* in the [Information for Authors](#).

Please note that technical editing may introduce minor changes to the text and/or graphics, which may alter content. The journal's standard [Terms & Conditions](#) and the [Ethical guidelines](#) still apply. In no event shall the Royal Society of Chemistry be held responsible for any errors or omissions in this *Accepted Manuscript* or any consequences arising from the use of any information it contains.

Cite this: DOI: 10.1039/c0xx00000x

www.rsc.org/xxxxxx

ARTICLE TYPE

Influence of the synthesis route on the 12R /10H-polytypes formation and their magnetic properties within the Ba(Ce,Mn)O₃ family

Mario A. Macías^a, Olivier Mentré^b, Caroline Pirovano^b, Pascal Roussel^b, Silviu Colis^c and Gilles H. Gauthier^{d*}

^a Universidad Industrial de Santander, Escuela de Química, GIQUE, Carrera 27, Calle 9, Ciudad Universitaria, Bucaramanga, Colombia.

^b Université Lille Nord de France, Unité de Catalyse et de Chimie du Solide, Equipe Chimie du Solide, Avenue Dimitri Mendeleïev, Bâtiment C7, ENSCL/UST Lille 1, BP 90108, 59652 Villeneuve d'Ascq Cedex, France.

^c Institut de Physique et Chimie des Matériaux de Strasbourg (IPCMS), UMR 7504 UDS-CNRS (UDS-ECPM), 23 rue du Loess, BP 43, F-67034 Strasbourg Cedex 2, France.

^d Universidad Industrial de Santander, Grupo INTERFASE, Carrera 27, Calle 9, Ciudad Universitaria, Bucaramanga, Colombia.

Received (in XXX, XXX) Xth XXXXXXXXXX 20XX, Accepted Xth XXXXXXXXXX 20XX

DOI: 10.1039/b000000x

The influence of Mn precursor on the polytypes formation was studied within the Ba-Ce-Mn-O system. Minor changes in the mean oxidation state of Mn cations guide the reaction route through different pathways obtaining the iso-stoichiometric 12R-Ba₄CeMn₄O_{12-δ} or 10H-Ba₅Ce_{1.25}Mn_{3.75}O_{15-δ} compounds. This behaviour was controlled using MnO₂ or MnCO₃ as starting chemical precursors. The understanding of such tendency allowed the synthesis of the new 10H-Ba₅Ce_{0.83}Mn_{4.17}O_{15-δ} composition through a two-step reaction route. This compound crystallizes in the hexagonal symmetry with space group *P63/mmc* (No-194) and cell parameters *a* = *b* = 5.77650(6) Å and *c* = 23.8590(4) Å. Its main characteristic stands in the presence of pure [Mn₄O₁₅] oligomers, establishing a difference with respect to the already known 10H-Ba₅Ce_{1.25}Mn_{3.75}O₁₅ polytype for which the principal feature was a mixed metal-occupancy within [Ce_{0.25}Mn_{3.75}O₁₅] tetramers. Such a difference generates strong antiferromagnetic (AFM) exchanges, contrary to the metamagnetic-like transition observed in 10H-Ba₅Ce_{1.25}Mn_{3.75}O₁₅. It is concluded that full Mn occupancy in [Mn₃O₁₂] or [Mn₄O₁₅] sub-units induce a robust AFM character.

KEYWORDS. Hexagonal perovskite, Precursors influence, Cation ordering, Manganite, Antiferromagnetism.

Introduction

The fascinating properties of transition metal compounds, particularly manganese oxides, have attracted the attention of many research groups during the last decades mainly because of their potential technological applications in the fields of heterogeneous catalysis,¹ Li-battery,^{2, 3} SOFC (Solid Oxide Fuel Cell) electrode materials,⁴ magnetic⁵ and also CMR (Colossal Magnetoresistance) materials.⁶ Among the structural possibilities, perovskite-type oxides form a family that also show such diversity. The ideal ABO₃ formula can yield two extreme close-packing types of AO₃ layers where the B cations occupy the octahedral holes, the cubic-*c*) (*abcabc*)⁷ and hexagonal-*h*) (*abab*) stacking sequences.⁸ Between these two extreme forms, it is possible to find a multitude of intermediate structures with sizable proportions of *c* and *h* layers.⁹ This is the case in the

Ba(Ce,Mn)O₃ series, in which Fuentes *et al.*¹⁰ tried to prepare several compounds of different Ce/Mn ratios and stacking sequences: 1/5 (Ba₆CeMn₅O₁₈), 1/4 (Ba₅CeMn₄O₁₅), 1/3 (Ba₄CeMn₃O₁₂), 1/2 (Ba₃CeMn₂O₉) and 1/1 (Ba₂CeMnO₆), all of them on the line of the phase diagram connecting *C*-BaCeO₃ to 2*H*-BaMnO₃.¹⁰ Nevertheless, only a 12*R*-Ba₄CeMn₄O₁₂ variety had been obtained as nearly pure and well ordered polytype, for which only the structural parameters have been described without any report of physical property measurements. In spite of the apparent impossibility to obtain a (*cchhh*)₂ stacking sequence with the formation of [Mn₄O₁₅] tetramers alternated by [CeO₆] octahedra along the *c*-axis into an hypothetical 10*H*-Ba₅CeMn₄O₁₅ structure,¹⁰ isotopic examples have been reported in similar systems, such as Ba₅In_{0.93}Mn₄O_{14.40},¹¹ Ba₅Sn_{1.1}Mn_{3.9}O₁₅¹² and Ba₅Sb_{1-x}Mn_{4+x}O_{15-δ},¹³ for which the necessity of cationic non-stoichiometry to get pure samples is worth noting. Recently, the crystal structure and magnetic

behavior of a new 10*H*-Ba₅Ce_{1.25}Mn_{3.75}O₁₅ polytype was reported.¹⁴ As described, in attempts to obtain the corresponding Ba₄CeMn₄O₁₂ compound, a change in the original reagents mixture induced the unexpected formation of [Ba₄CeMn₃O₁₂]_{5/4} ↔ Ba₅Ce_{1.25}Mn_{3.75}O₁₅, a new 10*H*-polytype in this family. Although the precursor's implication was undoubtful, such behavior had not been completely understood.

Concerning the physical properties of such materials, the structural arrangement of manganese cations in a pseudo one-dimensional compound is generally associated to strong antiferromagnetic (AFM) interactions within the face-sharing oligomers, but not to systematic long range interactions between them, as described for Ba₅In_{0.93}Mn₄O_{14.40},¹¹ Ba₄PrIr₃O₁₂,¹⁴ and Ba₄InMn₃O_{11.5}.¹⁶ However, an interesting magnetic behavior has been reported by Yin *et al.*¹² in such hexagonal perovskite-like oxides, where the Ba₅Sn_{1.1}Mn_{3.9}O₁₅ showed a spin glass transition at 7 K. Similarly, the 10*H*-Ba₅Sb_{1-x}Mn_{4+x}O_{15-δ} solid solution (0.24 < *x* < 0.36) presents a variation of magnetic properties that can be controlled by the *x* content of Mn in the corner-sharing Sb sites.¹³ In the Ba-Ce-Mn-O system, the recently reported 10*H*-Ba₅Ce_{1.25}Mn_{3.75}O₁₅ polytype¹⁴ showed evidence for strong AFM interactions already set at room temperature. An interesting metamagnetic-like transition was observed at around 50 K as a consequence of the magnetically isolated tetramers of face-sharing octahedra.

Based on such information, our attention was focused on a better understanding of the synthesis parameters that can selectively lead to the 10*H* or 12*R* polytype in the Ba-Ce-Mn-O system. The preparation of a new compound is also described, for which, along with the 12*R*-Ba₄CeMn₄O₁₂ polytype, the magnetic behavior is compared to the former 10*H* case of the series.

Experimental

In a previous work,¹⁴ the synthesis of 10*H*-Ba₅Ce_{1.25}Mn_{3.75}O₁₅ polytype has been described. This compound was obtained starting from a mixture BaCO₃/MnCO₃/CeO₂ = 4/3/1, which corresponds as well to the same stoichiometry that yields to the 12*R*-Ba₄CeMn₃O₁₂ structure. However, in order to obtain the 12*R*-Ba₄CeMn₃O₁₂ structure a BaCO₃/MnO₂/Ce₂(CO₃)₃ mixture was used.¹⁰ In a first step, with the aim to study such behavior, the synthetic routes were reproduced starting from the following mixtures of precursors:

Mixture 1 (M1): BaCO₃/MnO₂/Ce₂(CO₃)₃ with molar ratio (4/3/0.5)

Mixture 2 (M2): BaCO₃/MnCO₃/CeO₂ with molar ratio (4/3/1)

In both cases the synthesis was carried out by conventional solid-state reaction. M1 and M2 mixtures were ground in an agate mortar and pressed into pellets using the following precursors: BaCO₃ (Alfa Aesar 99.95%), MnO₂ or MnCO₃ (Alfa Aesar 99.9% and 99.985%) and Ce₂(CO₃)₃ or CeO₂ (Alfa Aesar 99.9 and 99.95%). Iterative heat treatments were further carried out in the range of 1000-1350 °C for 172 h in air with intermediate grinding/pelletizing to ensure a correct homogeneity of the sample. In each case, the reaction conditions were kept identical,

i.e. exactly the same steps were carefully followed for each mixture, including the thermal treatment using the same furnace. The solid state reactions were followed by X-ray powder diffraction at each intermediate temperature recording the corresponding data at room temperature.

As described below, aiming to prepare a hypothetical polytype of Ba₆CeMn₅O₁₈ composition, the new isostoichiometric 10*H*-Ba₅Ce_{0.83}Mn_{4.17}O₁₅ compound was obtained using the following route. Initially, an amount of pure Ba₆Mn₅O₁₆ compound was synthesized as polycrystalline sample by heating stoichiometric amounts of BaCO₃ (Alfa Aesar 99.95%) and MnO₂ (Alfa Aesar 99.985%) in air in the range of 1000-1200 °C for approximately 60 h. The latter product was used as starting precursor in the second step that consists of mixing Ba₆Mn₅O₁₆ with Ce₂(CO₃)₃ (Alfa Aesar 99.9%) as cerium source to obtain the corresponding targeted Ba/Mn/Ce=6/5/1 composition, then heating the mixture in the range of 1200-1450 °C for 94 h. Intermediate X-ray powder diffraction (XRPD) measurements were performed until no changes in the diffractograms were observed.

The XRPD patterns obtained in each step of this work were measured on a Bruker D8 diffractometer operated in Bragg-Brentano geometry, equipped with a Ni filter, a beam of CuKα_{1,2} radiation (λ=1.540598 and 1.54439 Å) and a one-dimensional LynxEye detector. The patterns were collected at room temperature in the 2θ range of 10°–120° using a 2θ step size of 0.0153°.

The data analysis was performed by the Rietveld method using the Jana-2006 program.¹⁷ The process of refinements was carried out assuming a pseudo-Voigt function for peak shape and a calculated background using a linear interpolation between a set of fixed points.

The field and temperature dependent magnetic measurements were carried out using a Quantum Design SQUID-VSM magnetometer. The temperature dependence variation of the magnetization was carried out under a magnetic field of 0.1 T after cooling the sample in a field of 0.1 T (FC, field cooling) or in zero field (ZFC, zero field cooling).

Results and Discussion

Study of the selectively in the route to 12*R*/10*H* polytypes

In our previous work dealing with the synthesis of 10*H*-Ba₅Ce_{1.25}Mn_{3.75}O₁₅ polytype, combined structure refinement of X-ray and neutron diffraction data has been used to prove that the compound crystallizes in a (*cchhh*)₂ sequence (instead of the (*hhhc*)₃ sequence of the iso-stoichiometric 12*R*-Ba₄CeMn₃O₁₂), in which the principal feature is the formation of face-sharing octahedral [Ce_{0.25}Mn_{3.75}O₁₅] tetramers that share corners with [CeO₆] octahedra, forming chains along *c*-axis.¹⁴ Summarizing our previous findings, the only evidence concerning the synthetic divergence corresponds to the fact that, apparently, the mixture of precursors might be responsible for the slight change in the reaction routes leading predominantly to the 12*R* or 10*H* polytypes. As observed in Fig. 1, the diffraction patterns of both samples (M1, *i.e.* BaCO₃/MnO₂/Ce₂(CO₃)₃ with Ba/Mn/Ce molar

ratio (4/3/1), and M2, i.e. BaCO₃/MnCO₃/CeO₂ with the same molar ratio), present an unexpected behavior: from the first steps of the synthesis (T~1000 °C), a clear influence of the reagents on the amounts of intermediate products can be observed. To examine the development of the reaction process, each diffractogram was initially analyzed using the Inorganic Crystal Structure Database (ICSD) to corroborate the identity of the formed phases: Ba₄Mn₃O₁₀, Ba₆Mn₅O₁₆, BaCeO₃, BaMnO₃, CeO₂ and a 12R-Ba₄CeMn₃O₁₂-type compound were identified. Afterwards, a quantitative procedure was carried out using the Rietveld method¹⁸ (Table 1).

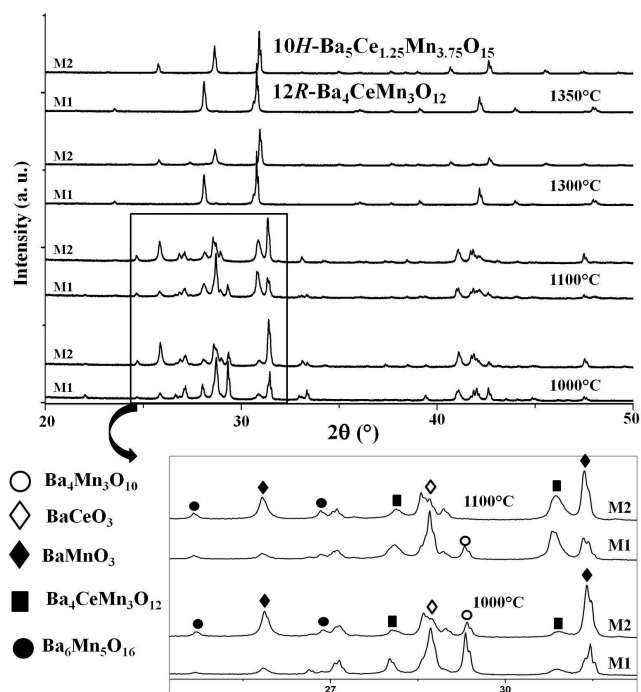


Fig. 1. X-ray diffraction sequence as a function of temperature. The reactions are taking different routes when M1 and M2 reagent mixtures are used.

From Fig. 1 and Table 1, it is possible to deduce that, in both cases, the same phases are present at intermediate temperatures, but with different amounts of each one. At 1000 °C, a deviation in the pathways emerges with the formation, preferentially, of Ba₄Mn₃O₁₀ and BaCeO₃ as major components in M1. Meanwhile, in M2, the chemical behaviour leads to the preferred formation of Ba₆Mn₅O₁₆ and BaMnO₃ compounds. Such a tendency is confirmed following the treatment at 1100 °C, for which the formation of Ba₆Mn₅O₁₆ and BaMnO₃ is clearly favoured in M2. In the case of M1, in spite of the fact that an increment in the amount of Ba₆Mn₅O₁₆ is observed, the amount of BaMnO₃ remains low and a preference for Ba₄Mn₃O₁₀ and BaCeO₃ is still detected when compared to M2. Moreover, considering the already known crystal structure of both 12R and 10H compounds, the Rietveld analysis shows that, at 1000 and 1100 °C, the only detected polytype is 12R in both samples, and that, at 1100 °C, it is already in higher amounts in M1 than in M2. At 1300 °C, the difference is undoubtful and the formation of only one polytype is

clearly observed, 12R or 10H that depends on the reagent mixture M1 or M2, respectively.

To understand the behavior observed following these synthetic routes it is worth noting that the 2H-BaMnO₃ compound is build up by a hexagonal stacking of BaO₃ layers where the Mn cations are occupying the octahedral sites, leading to infinite chains of MnO₆ face-sharing octahedra along the *c*-axis.¹⁹ On the other hand, the Ba₆Mn₅O₁₆ compound,²⁰ isotopic to Cs₆Ni₅F₁₆,²¹ is formed by [Mn₅O₁₈] units of five face-sharing octahedra. These units are connected via their apices by sharing two of their terminal corners. Following this order, the Ba₄Mn₃O₁₀ compound,²² isotopic to Cs₄Ni₃F₁₀,²³ is build up from [Mn₃O₁₂] units of three face-sharing octahedra linked also by their apices. The essential difference between those structures relies in the length of their Mn-oligomers and the way in which they are connected: infinite chains for 2H-BaMnO₃ and 5 to 3 octahedral units per oligomer in Ba₆Mn₅O₁₆ and Ba₄Mn₃O₁₀, respectively. This observation allows to suppose that M2 mixture can influence the formation of long-chains based compounds which hypothetically favor the stabilization of 10H-polytypes in the Ba-Ce-Mn-O system. Remembering the first synthesis of 12R-Ba₄CeMn₃O₁₂ by Fuentes *et al.*,¹⁰ the starting mixture employed was BaCO₃/MnO₂/CeO₂. Considering M1 and M2 mixtures used in this work, it is possible to confirm a direct influence of the Mn source in the synthetic orientation. This argument is not a surprise considering the recent work of Iorgulescu *et al.*²⁴⁻²⁵ According to this study, the size of individual hexagonal-perovskite blocks, either trimeric (*n*=3) or tetrameric (*n*=4) layers of *n* face-sharing octahedra, can be controlled by the mean oxidation number of the transition metal in the Ba(Co₃M)X_{0.2-x}O_{3-δ} (X=F, Cl; M=Fe, Mn) series. It was demonstrated that Fe incorporation into the Co structure stabilizes exclusively a 10H-form for which the lowest content of hexagonal layers stemmed from a metal reduction along with the increase of Fe/Co ratio. On the contrary, the influence of Mn substitution was to increase the mean (Co/Mn) valence, stabilizing the 6H-form with tetramers of face-sharing octahedra.

Table 1. Quantitative (wt%) phase analysis using the Rietveld method for M1 and M2 mixtures heat treated at 1000 and 1100 °C.

Compound	Mixture 1 (wt%)		Mixture 2 (wt%)	
	1000 °C	1100 °C	1000 °C	1100 °C
Ba ₄ Mn ₃ O ₁₀	38.0(4)	14.4(4)	14.1(5)	1.4(2)
Ba ₆ Mn ₅ O ₁₆	11.5(5)	22.7(6)	25.5(6)	27.6(5)
BaCeO ₃	22.6(4)	19.6(4)	7.7(3)	9.4(3)
BaMnO ₃	6.5(2)	5.5(2)	23.7(4)	23.2(4)
CeO ₂	10.2(3)	6.7(4)	17.9(4)	19.8(4)
Ba ₄ CeMn ₃ O ₁₂	11(1)	31(1)	11(1)	18(1)
R _w	0.049	0.053	0.049	0.051
R _{exp}	0.029	0.027	0.027	0.036
χ ²	1.7	1.9	1.9	1.9

The arguments presented so far suggest that under the preparation conditions, the mean oxidation state of the Mn cations might change during the de-carbonation process when MnCO_3 is used. As it is known, the thermal decomposition in air leads to the conversion of MnCO_3 into MnO_2 , Mn_2O_3 or Mn_3O_4 , which not only depends on the temperature but also on the partial pressure of oxygen and/or CO_2 .²⁶ In order to determine the mean valence of the Mn cations within the $12R$ and $10H$ polytypes, a redox titration was performed on each compound. Taking into account the estimated precision of the iodometric titration ($\sim 2\text{-}3\%$), our results did not show any clear difference between the $12R$ and $10H$ compounds, leading in all cases to a mean $4+$ oxidation state for both Ce and Mn cations, in agreement with previous works in the series.^{10, 14} Nevertheless, it is worth mentioning that the structural divergence might be controlled by very small changes in the oxidation state of Mn ions. Such behavior has been well reviewed recently in the BaMnO_{3-x} series in which several polytypes have been observed: $2H$ - BaMnO_3 (Mn^{4+}), $15R$ - $\text{BaMnO}_{2.99}$ ($\text{Mn}^{3.98+}$), $8H$ - $\text{BaMnO}_{2.95}$ ($\text{Mn}^{3.90+}$), $6H$ - $\text{BaMnO}_{2.92}$ ($\text{Mn}^{3.84+}$), $10H$ - $\text{BaMnO}_{2.91}$ ($\text{Mn}^{3.82+}$) and $4H$ - $\text{BaMnO}_{2.65}$ ($\text{Mn}^{3.30+}$).²⁷

Searching for new polytypes in the $\text{Ba}_{n+1}\text{CeMn}_n\text{O}_{3n+3}$ series

As mentioned above,¹⁰ efforts to obtain other members of the $\text{Ba}_{n+1}\text{CeMn}_n\text{O}_{3n+3}$ series with $n=5$ ($\text{Ba}_6\text{CeMn}_5\text{O}_{18}$), 4 ($\text{Ba}_5\text{CeMn}_4\text{O}_{15}$), 2 ($\text{Ba}_3\text{CeMn}_2\text{O}_9$), or 1 ($\text{Ba}_2\text{CeMnO}_6$), i.e. different to the already known $n=3$ ($\text{Ba}_4\text{CeMn}_3\text{O}_{12}$) $12R$ -polytype, resulted in failed endings.¹⁰ The only exception corresponds to the recent published $10H$ - $\text{Ba}_5\text{Ce}_{1.25}\text{Mn}_{3.75}\text{O}_{15}$ polytype.¹⁴ As a consequence, and with the aim to corroborate the precursors influence on the synthetic route, we decided to prepare new compounds that would contain tetramers or even pentamers, like would be the case of $\text{Ba}_5\text{CeMn}_4\text{O}_{15}$ and $\text{Ba}_6\text{CeMn}_5\text{O}_{18}$. For the former composition, different attempts were carried out considering not only the use of MnCO_3 as the source of manganese, but also starting from $\text{Ba}_6\text{Mn}_5\text{O}_{16}$ as precursor, taking into account the intermediate formation of such pentamer-based barium manganite in the way to $10H$ -polytype (see Table 1). However, all our efforts failed, leading to mixtures of $12R$ ($a \sim 5.79 \text{ \AA}$ and $c \sim 28.60 \text{ \AA}$) and $10H$ ($a \sim 5.78 \text{ \AA}$ and $c \sim 23.87 \text{ \AA}$) polytypes, including low proportions of $\text{Ba}_3\text{Mn}_2\text{O}_8$ and $\text{Ba}_4\text{Mn}_3\text{O}_{10}$ secondary phases. All attempts to obtain a pure $10H$ -sample were frustrated by the presence of the $12R$ -polytype, as if the exactly stoichiometric composition were thermodynamically unstable in the range of temperature that has been considered in air. At this stage, it is worth noting that all other existing examples of $10H$ -isotypic structures, i.e. $\text{Ba}_5\text{In}_{0.93}\text{Mn}_4\text{O}_{14.40}$, $\text{Ba}_5\text{Sn}_{1.1}\text{Mn}_{3.9}\text{O}_{15}$, $\text{Ba}_5\text{Sb}_{1-x}\text{Mn}_{4+x}\text{O}_{15-\delta}$ ($0.24 \leq x \leq 0.36$) and $\text{Ba}_5\text{Ce}_{1.25}\text{Mn}_{3.75}\text{O}_{15}$,¹¹⁻¹⁴ are systematically out of the exact $\text{Ba}_{n+1}\text{MMn}_n\text{O}_{3n+3}$ stoichiometry (understoichiometric composition for trivalent M cations as In^{3+} or Sb^{3+} and overstoichiometric for tetravalent cations as Ce^{4+} or Sn^{4+} , with respect to the ideal stoichiometry of the $n=4$ member). As far as we know, no explanation of such feature has been given. However, based on the consideration detailed above, a hypothesis would be to consider the importance to stabilize a particular oxidation state for Mn in order to guide the synthesis to the formation of the $10H$ -polytype. It seems that such control can be reached by a

correct balance of the $\text{M}^{3+/4+}$ to Mn ratio.

The attempts to synthesize the $n=5$ member of the series with $\text{Ba}_6\text{CeMn}_5\text{O}_{18}$ composition provided better results. In this case, and as described in Fig. 2, a pure phase was formed using a two-step synthesis. Indeed, based on the results described above, the stabilization of a structure built up from tetramers was obtained by the prior synthesis of the $\text{Ba}_6\text{Mn}_5\text{O}_{16}$ intermediate, a structure made of $[\text{Mn}_5\text{O}_{18}]$ units of face-sharing octahedra.²⁰ After this first step, a stoichiometric amount of $\text{Ce}_2(\text{CO}_3)_3$ precursor was weighted, carefully mixed with the barium manganite and ground in an agate mortar, pressed into pellets and finally heated in a range of temperature from 1000 to $1400 \text{ }^\circ\text{C}$ for 172 h in air, with intermediate grindings. As a result, a diffractogram similar to that observed for $\text{Ba}_5\text{Ce}_{1.25}\text{Mn}_{3.75}\text{O}_{15}$ ¹⁴ was obtained, that suggests that the $6:1:5$ composition, hypothetically pentameric ($n=5$) structure, could have crystallized, in fact, in a tetrameric ($n=4$) ($cchhh$)₂ sequence.

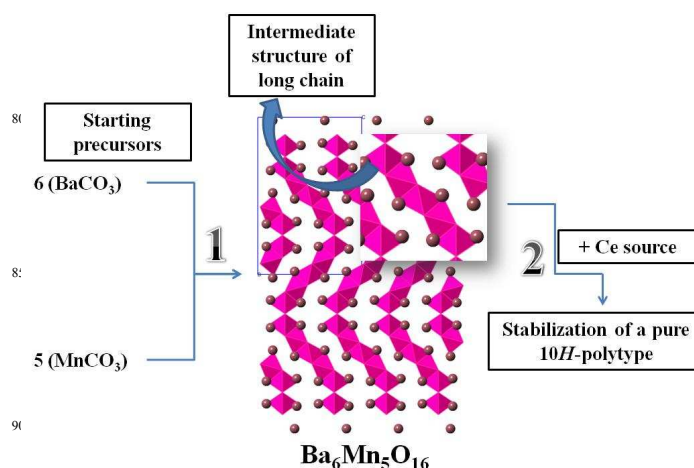


Fig. 2. $10H$ -polytype stabilization using a 2-step method.

To confirm such assumption, the X-ray diffraction pattern for this new composition was analyzed. The observed peaks were indexed in a hexagonal unit cell with $a = b = 5.77650(6) \text{ \AA}$ and $c = 23.8590(4) \text{ \AA}$, and most probable space group $P63/mmc$ (No. 194) according to the reflexion conditions.²⁹ As mentioned for the $10H$ - $\text{Ba}_5\text{Ce}_{1.25}\text{Mn}_{3.75}\text{O}_{15}$ polytype of the family,¹⁴ the c -value confirms a $10H$ -structure, considering the $c \sim n \cdot 2.38 \text{ \AA}$ condition. After a complete analysis using the Le Bail method,³⁰ a pure phase was confirmed. The crystal structure was assumed isotypic to the previous $10H$ -polytype,¹⁴ so the Rietveld analysis was initiated, taking into account a complete Mn-occupation into the tetramers, in agreement with the exact stoichiometry. Indeed, other attempts of refinements were performed, considering a possible Mn/Ce mixed occupancy into the tetramers, but the analysis of the atomic displacement parameters (ADP) suggest the formation of pure $[\text{Mn}_4\text{O}_{15}]$ oligomers. The final crystal structure parameters are summarized in Table 2, whereas Table 3 shows some selected inter-atomic distances for this new material, whose composition must in fact be rewritten as $[\text{Ba}_6\text{CeMn}_5\text{O}_{18}]_{5/6} = \text{Ba}_5\text{Ce}_{0.83}\text{Mn}_{4.17}\text{O}_{15}$.

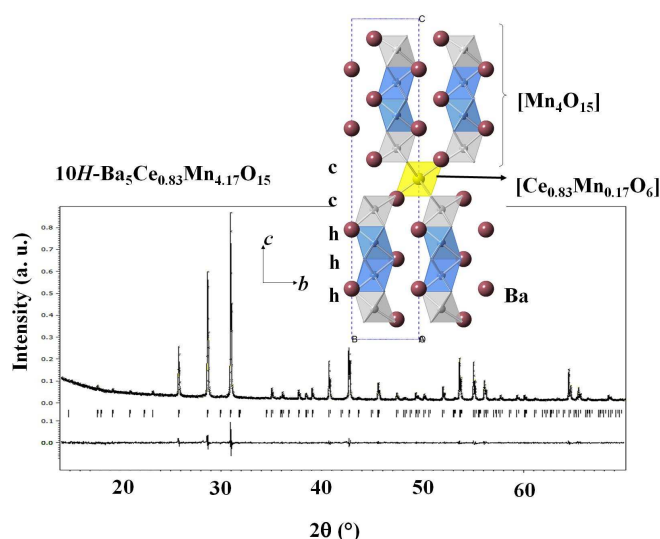


Fig. 3. Rietveld analysis using XRPD data confirming that the $\text{Ba}_5\text{Ce}_{0.83}\text{Mn}_{4.17}\text{O}_{15}$ compound is isotopic to $10H\text{-Ba}_5\text{Ce}_{1.25}\text{Mn}_{3.75}\text{O}_{15}$.

The main structural feature of this compound is thus the formation of $[\text{Mn}_4\text{O}_{15}]$ face sharing octahedral tetramers that in turn share corners with $[\text{Ce}_{0.83}\text{Mn}_{0.17}\text{O}_6]$ octahedra, describing thus zig-zag chains along c -axis. Fig. 3 shows the comparison of observed and calculated patterns obtained from the Rietveld analysis in which no additional peaks were observed, indicating a perfectly ordered intergrowth of cubic and hexagonal layers, establishing a difference with the other two members of the family for which the presence of ceria had been detected.^{10, 14} This observation confirms Fuentes *et al.*'s predictions about the possible existence of ordered polytypes when an adequate composition can be achieved by adjusting the thermodynamic conditions.¹⁰

Table 2. Final crystal structure parameters for $\text{Ba}_5\text{Ce}_{0.83}\text{Mn}_{4.17}\text{O}_{15}$ obtained from Rietveld refinement using XRPD data.

Atom	Site	x, y, z	$U_{\text{iso}} (\text{\AA}^2)$	Occupancy
Ba1	2d	$2/3, 1/3, 1/4$	0.012(5)	1.0
Ba2	4f	$2/3, 1/3, 0.4395(2)$	0.012	1.0
Ba3	4e	$0, 0, 0.3422(2)$	0.012	1.0
Ce1	2a	$0, 0, 1/2$	0.010(4)	0.83
Mn1	2a	$0, 0, 1/2$	0.010	0.17
Mn2	4f	$1/3, 2/3, 0.3021(5)$	0.010	1.0
Mn3	4f	$1/3, 2/3, 0.4064(5)$	0.010	1.0
O1	6h	$0.188(4), 0.812(4), 1/4$	0.020(6)	1.0
O2	12k	$0.167(3), 0.334(3), 0.448(1)$	0.020	1.0
O3	12k	$0.481(2), 0.962(2), 0.3491(8)$	0.020	1.0

Table 3. Selected bond distances (\AA) for $\text{Ba}_5\text{Ce}_{0.83}\text{Mn}_{4.17}\text{O}_{15}$.

Ba1-O1	2.90(3) x6	(Ce1/Mn1)-O2	2.08(2) x6
Ba1-O3	3.00(2) x6	Mn3-O2	1.94(3) x3
Ba2-O2	2.90(2) x6	Mn3-O3	2.02(2) x3
Ba2-O2	3.16(3) x3	Mn2-O1	1.91(2) x3
Ba2-O3	2.84(2) x3	Mn2-O3	1.86(2) x3
Ba3-O1	2.89(2) x3	Mn2'-Mn2	2.49(2)
Ba3-O2	3.02(2) x3	Mn3-Mn2	2.49(2)
Ba3-O3	2.90(3) x6	(Ce1/Mn1)-Mn3	4.014(8)

The calculated $\text{Mn}^{4+}/\text{Ce}^{4+}$ distribution for this structure becomes evident when the inter-atomic distance (Ce1/Mn1)-O2 (2.08(2) \AA) is compared with the corresponding value Ce1-O2 (2.19(2) \AA) reported for $10H\text{-Ba}_5\text{Ce}_{1.25}\text{Mn}_{3.75}\text{O}_{15}$.¹⁴ The difference between cationic radii makes therefore shorter the distance in the present case.

50 Thermal relationship between 12R and 10H polytypes

The evidence collected so far establishes solid bases supporting the influence of the Mn-source on the synthesis route which is not a common occurrence in solid state chemistry. An example of structural transition between the same tetramer- and trimer-containing 10H- and 12R-polytypes has been already observed in the Cs-Ni-Cd-F system. In this case, $12R\text{-Cs}_4\text{Ni}_3\text{CdF}_{12}$ shows a temperature-induced polymorphic transformation to $10H\text{-Cs}_5\text{Ni}_{3.75}\text{Cd}_{1.25}\text{F}_{15}$ above 850°C .³¹ With the aim to examine if a similar behavior could also occur in our case, a high temperature thermal treatment was carried out on $10H\text{-Ba}_5\text{Ce}_{1.25}\text{Mn}_{3.75}\text{O}_{15}$. The sample was heated at 1500°C for 4 h in air, *i.e.* a much higher temperature in comparison to the synthesis conditions ($T=1350^\circ\text{C}$).

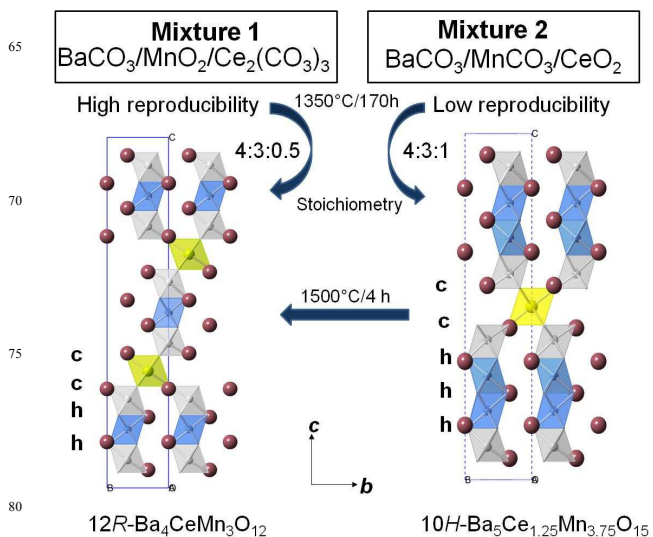


Fig. 4. Schematic representation of the influence of precursor and temperature on the nature of the polytype obtained within the Ba-Ce-Mn-O system.

The XRD analysis showed that the 10H-polytype was totally transformed into a 12R-polytype. The cell parameters of the latter compound, $a = b = 5.7948(1) \text{\AA}$ and $c = 28.5746(6) \text{\AA}$, are close

from those reported for $\text{Ba}_4\text{CeMn}_3\text{O}_{12}$ ($a=5.7980(1)$ Å, $c=28.6070(8)$ Å).¹⁰ Based on the previously described cases of $\text{Ba}(\text{Co}/\text{M})\text{X}_{0.2-3}\text{O}_{3-\delta}$ ($\text{X}=\text{F}, \text{Cl}; \text{M}=\text{Mn}, \text{Fe}$)²⁴⁻²⁵ or $\text{BaMnO}_{3-\delta}$ polytypes,²⁷ it is possible to imagine a similar relationship between $10H\text{-Ba}_5\text{Ce}_{1.25}\text{Mn}_{3.75}\text{O}_{15}$ and $12R\text{-Ba}_4\text{CeMn}_3\text{O}_{12}$, *i.e.* a phase transition that could be controlled by a slight change in the mean oxidation state of the Mn cations. This is summarized in Fig. 4. Several attempts to identify such structural transition by TGA/DTA were unsuccessful, suggesting that the difference of Mn oxidation state must be very small, if our hypothesis is true. In a similar way, the thermal treatment of the new composition $10H\text{-Ba}_5\text{Ce}_{0.83}\text{Mn}_{4.17}\text{O}_{15}$ also produced the same behavior, for which a temperature-driven tetramer to trimer transformation was also observed.

Magnetic properties of $12R\text{-Ba}_4\text{CeMn}_3\text{O}_{12}$ and $10H\text{-Ba}_5\text{Ce}_{0.83}\text{Mn}_{4.17}\text{O}_{15}$ structures

The magnetic properties of both $12R\text{-Ba}_4\text{CeMn}_3\text{O}_{12}$ and $10H\text{-Ba}_5\text{Ce}_{0.83}\text{Mn}_{4.17}\text{O}_{15}$ compounds have been investigated by means of magnetization versus temperature measurements. The complex magnetic properties inherent to manganese-based hexagonal perovskites have already been described in several works,^{11-13, 27} and resumed in our prior study on $\text{Ba}_5\text{Ce}_{1.25}\text{Mn}_{3.75}\text{O}_{15}$.¹⁴ In substance, it appears that systems that possess a significant amount of Mn^{3+} states within the mixed $\text{Mn}^{3+}/\text{Mn}^{4+}$ valence generally show a Curie-Weiss behavior below room temperature followed by several kinds of antiferromagnetic-like 3D orderings on further cooling, *e.g.* in $\text{Ba}_5\text{Sb}_{1-x}\text{Mn}_{4+x}\text{O}_{15-\delta}$ ¹³ or $\text{Ba}_6\text{Co}_2\text{Mn}_4\text{ClO}_{16-\delta}$ oxochloride.²⁵ On the opposite, a majority of Mn^{4+} ions generally leads to non-Curie-weiss behaviors until room temperature which most probably pictures strongest AFM exchanges, leading to short range ordering at appreciably high temperature. It is clear that in addition, the competition between Mn-O-Mn exchanges is expected stronger between $\text{Mn}^{4+}\text{-d}3$ cations ($t_{2g}^3 e_g^0$) than between Mn^{3+} ($t_{2g}^3 e_g^1$) since $e_g\text{-O}_{2p}\text{-}e_g$ and $t_{2g}\text{-O}_{2p}\text{-}t_{2g}$ generally lead to opposite signs of exchanges.³² The interplay between the different exchanges is complicated by the geometry of hexagonal perovskites which combine several magnetic couplings such as between columns inside the sheets, between the chains (interchain) or between ions inside the chains (intrachain). For instance in the series of hexagonal $\text{BaMnO}_{3-\delta}$ polytypes revisited by Adkin *et al.*,²⁷ it was shown that the temperature of magnetic ordering in each phase increases steadily with the fraction of cubic layers (x) within the structures. This observation was often justified using the idea that the strong antiferromagnetic coupling between spins is mediated by the strong (90°) Mn-O-Mn links in the columns, which are formed by the face-sharing of MnO_6 octahedra, with full three-dimensional ordering occurring only when the weaker (180°) Mn-O-Mn superexchange pathway formed by the corner sharing of MnO_6 octahedra can overcome thermal scattering.^{27, 33, 34} This image is probably to be revised since Kanamori-Goodenough rules unambiguously predict strong FM 90° $\text{Mn}^{4+}\text{-O-Mn}^{4+}$ exchanges, and direct AFM $\text{Mn}^{4+}\text{-Mn}^{4+}$ exchanges are most probably involved. For $4H\text{-(Ba,Sr)MnO}_3$ compounds with an equivalent density of face-sharing and corner-sharing (180°) paths, direct exchanges are effective at room temperature, while the 3D ordering (ZFC/FC divergence) is brought at 260K between

columns by the 180° exchanges.³⁴ The strength of the inter-chain couplings is responsible for the magnetic ordering at relatively high temperature ($T_N \sim 59\text{K}$) in the $2H\text{-BaMnO}_3$ in absence of cubic stacked (isolated columns of MnO_6 octahedra). Accordingly with the disposition of the columns in (*a*, *b*) triangular lattice such arrangement are presumably responsible for strong frustration and canted spin orientations.²⁷

The temperature dependence of the magnetic susceptibility χ and its inverse are shown in Fig. 5(a) and 5(b) for $\text{Ba}_4\text{Mn}_3\text{CeO}_{12}$ and $\text{Ba}_5\text{Mn}_{4.17}\text{Ce}_{0.83}\text{O}_{15}$, respectively. The magnetic behavior is similar for both compounds.

a) It was not possible to extract a consistent Curie-Weiss law since for both compounds we observe rounded $\chi^{-1}(T)$ shape reminiscent of short order interactions close to room temperature. Consideration of independent temperature paramagnetic term did not improve fit leading to meaningless physical values. For $\text{Ba}_4\text{Mn}_3\text{CeO}_{12}$ we obtain in the 300-400 K domain (nearly linear $\chi^{-1}(T)$ domain) $\mu_{\text{eff}} \sim 2.5$ $\mu\text{B}/\text{f.u.}$ and $\Theta_{\text{CW}} < -2000$ K. For $\text{Ba}_5\text{Mn}_{4.17}\text{Ce}_{0.83}\text{O}_{15}$ we obtain in the 200-360 K domain $\mu_{\text{eff}} \sim 1.8$ $\mu\text{B}/\text{f.u.}$ and $\Theta_{\text{CW}} < -2100$ K. It is far to explain the 6.71 $\mu\text{B}/\text{f.u.}$ and 7.91 $\mu\text{B}/\text{f.u.}$ calculated for paramagnetic Mn^{4+} ($S=3/2$) using a spin-only contribution. Also the huge negative values for Θ_{CW} , are not plausible. At least, they could picture strong AFM exchanges, in agreement with previous arguments for Mn^{4+} spins already strongly involved in robust AFM exchanges at room temperature.

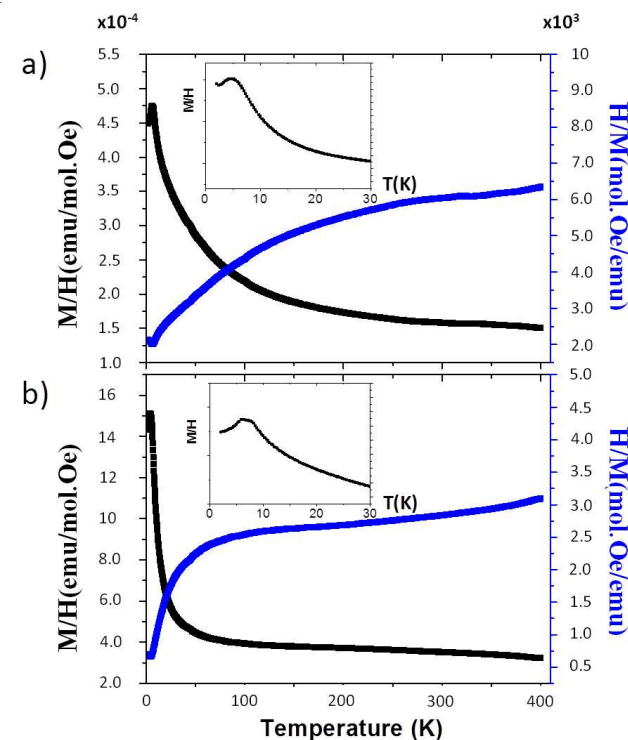


Fig. 5. Thermal evolutions of magnetic susceptibility χ and its inverse for (a) $\text{Ba}_4\text{Mn}_3\text{CeO}_{12}$ and (b) $\text{Ba}_5\text{Mn}_{4.17}\text{Ce}_{0.83}\text{O}_{15}$ compounds.

b) Both compounds show an inflection of $\chi^{-1}(T)$ around 350 K. A similar anomaly but more abrupt was already observed in

Ba₅Ce_{1.25}Mn_{3.75}O₁₅¹⁴ and most probably pictures the setting of short-range ordering AFM exchanges. The progressive decrease of $\chi^{-1}(T)$ below 300K and 100K for Ba₄Mn₃CeO₁₂ and Ba₅Mn_{4.17}Ce_{0.83}O₁₅ respectively, denote the expansion of AFM correlations in the crystal.

c) Finally, contrarily to Ba₅Ce_{1.25}Mn_{3.75}O₁₅,¹⁴ ZFC and FC data are fully convergent which refute the presence of weak (uncompensated) ferromagnetism, canted-spins or spin-glass like behavior. According to the ideal models discussed previously, either Mn⁴⁺₃O₁₂ or Mn⁴⁺₄O₁₅ sub-units are non-substituted and separated by corner-sharing diamagnetic Ce⁴⁺O₆ or mixed Ce/Mn sites. It makes the difference with Ba₅Ce_{1.25}Mn_{3.75}O₁₅,¹⁴ in which tetramer columns were partially substituted and at the probable origin of the weak observed FM. In the two title compounds, the Néel-like anomaly observed around T=6 K plays in favor of a 3D AFM ordering via Mn-Ce-O-Mn bridges. It validates the importance of “integrity” of Mn_xO_{3x+3} units in the suppression of magnetic disorder, leading to full-moment cancellation.

Conclusions

We studied the Mn-precursor influence on the synthesis of the 12R/10H polytypes in the Ba-Ce-Mn-O family. According to our results, the use of MnO₂ or MnCO₃ as starting chemical precursors can guide the reaction routes through different paths which allow the formation of the 12R-Ba₄Mn₃CeO₁₂ or 10H-Ba₅Ce_{1.25}Mn_{3.75}O₁₅ compounds, respectively. This phenomenon was explained as an influence of the Mn mean oxidation state on the structural organization into trimeric (n=3) or tetrameric (n=4) polytypes, built upon [Mn_nO_{3n+3}] units. The study of intermediate phases formed during each synthesis route allowed the stabilization of the new 10H-Ba₅Mn_{4.17}Ce_{0.83}O₁₅ composition in a two-step reaction process. Through XRPD data we confirmed that this compound, isotypic to Ba₅Ce_{1.25}Mn_{3.75}O₁₅, crystallizes in a (cchhh)₂ sequence formed by face-sharing octahedral [Mn₄O₁₅] tetramers that share corners with [Ce_{0.83}Mn_{0.17}O₆] octahedra. Such a difference respecting to the prior 10H-polytype in which the tetramers were formed by mixed Ce/Mn sites, induce strong AFM exchanges which suggest that the “integrity” of the Mn_xO_{3x+3} units plays a role of suppression of the magnetic disorder in this kind of structures. This behavior was corroborated by the similar magnetic results obtained for the 12R-Ba₄Mn₃CeO₁₂ compound.

These results allow to conclude that even small changes in the mean oxidation state of the transitions metals (TM) can guide a synthesis route by different ways and lead to different polytypes. This behavior can be accomplished either by a correct choice of the precursors for the TM-source or, more classically, changing the TM mean valence by an adequate temperature and/or atmosphere control.

Acknowledgments

This work was developed with the financial support from the Vice-Rectorship for Research and Extension of the Universidad Industrial de Santander in the frame of the project # 5196 called “Síntesis, estudio estructural y propiedades magnéticas de nuevos materiales pertenecientes a los sistemas I2-II-IV-VI4 y Ba-R-M-O”. Mario A. Macías received a PhD grant from COLCIENCIAS.

The « Fonds Européen de Développement Régional (FEDER) », « CNRS », « Région Nord Pas-de-Calais » and « Ministère de l'Éducation Nationale de l'Enseignement Supérieur et de la Recherche » are acknowledged for funding of X-ray diffractometers and TEM facility.

References

- (1) Q. Feng, H. Kanoh, K. Ooi. *J. Mater. Chem.* **1999**, 9, 319-333.
- (2) P. Strobel, C. Mouget. *Mater. Res. Bull.* **1993**, 28, 93-100.
- (3) A.R. Armstrong, P.G. Bruce. *Nature* **1996**, 381, 499-500.
- (4) M. Mogensen, K.V. Jensen, M.J. Jørgensen, S. Primdahl. *Solid State Ionics* **2002**, 150, 123-129.
- (5) G. H. Jonker, J. H. Van Santen. *Physica* **1950**, 16, 337-349.
- (6) J.M. Longo, J.A. Kafalas. *J. Solid State Chem.* **1969**, 1, 103-108.
- (7) S. Colis, D. Stoeffler, C. Mény, T. Fix, C. Leuvrey, G. Pourroy, A. Dinia, and P. Panissod. *J. Appl. Phys.* **2005**, 98, 033905.
- (8) R.H. Buttner, E.N. Maslen. *Acta Crystallogr. B* **1992**, 48, 764-769.
- (9) M. Iorgulescu, H. Kabbour, N. Tancret, O. Mentré, P. Roussel. *Chem. Commun.* **2010**, 46, 5271-5273.
- (10) F. Fuentes, K. Boulahya, U. Amador. *J. Solid State Chem.* **2004**, 177, 714-720.
- (11) C. Yin, G. Li, T. Jin, L. You, J. Tao, J.W. Richardson, C. Loong, J. Sun, F. Liao, J. Lin. *Chem. Mater.* **2008**, 20, 2110-2116.
- (12) C. Yin, G. Li, T. Jin, J. Tao, J.W. Richardson, C.-K. Loong, F. Liao, J. Lin. *J. Alloys Compd.* **2010**, 489, 152-156.
- (13) C. Yin, G. Li, W.A. Kockelmann, F. Liao, J.P. Attfield, J. Lin. *Chem. Mater.* **2010**, 22, 3269-3276.
- (14) M.A. Macías, O. Mentré, S. Colis, G.J. Cuello, G.H. Gauthier. *J. Solid State Chem.* **2013**, 198, 186-191.
- (15) Y. Shimoda, Y. Doi, M. Wakeshima, Y. Hinatsu. *J. Solid State Chem.* **2010**, 183, 1962-1969.
- (16) X. Kuang, C. Bridges, M. Allix, J.B. Claridge, H. Hughes, M.J. Rosseinsky. *Chem. Mater.* **2006**, 18, 5130-5136.
- (17) V. Petricek, M. Dusek, L. Palatinus. **2006**. Jana2006. The crystallographic computing system. Institute of Physics, Praha, Czech Republic. <http://jana.fzu.cz/>
- (18) R.A. Young. *The Rietveld Method*. Oxford: IUCr, Oxford University Press, New York, United States, **1993**.
- (19) A. Hardy. *Acta Crystallogr.* **1962**, 15, 179-181.
- (20) K. Boulahya, M. Parras, J.M. González-Calbet, J.L. Martínez. *Chem. Mater.* **2002**, 14, 4006-4008.
- (21) R. Schmidt, D. Babel. *Z. Anorg. Allg. Chem.* **1984**, 516, 187-195.
- (22) V. Zubkov, A. Tyutyunnik, I.F. Berger, V.I. Voronin, G.V. Bazuev, C.A. Moore, P.D. Battle. *J. Solid State Chem.* **2002**, 167, 453-458.
- (23) R. Schmidt, J. Pebler, D. Babel. *Eur. J. Solid State Inorg. Chem.* **1992**, 29, 679.
- (24) M. Iorgulescu, P. Roussel, N. Tancret, N. Renault, F. Porcher, G. André, H. Kabbour, O. Mentré. *Inorg. Chem.* **2012**, 51, 7433-7435.
- (25) M. Iorgulescu, P. Roussel, N. Tancret, N. Renault, N.

-
- Tiercelin, O. Mentré. *J. Solid State Chem.* **2013**, 198, 210-217.
- (26) W.M. Shaheen, M.M. Selim. *Thermochimica Acta* **1998**, 322, 117-128.
- (27) J.J. Adkin, M.A. Hayward. *Chem. Mater.* **2007**, 19, 755-762.
- 5 (28) R.D. Shannon. *Acta Cryst. A.* **1976**, 32, 751-767.
- (29) International Tables for X-Ray Crystallography vol. A, Fifth ed., Springer, Heidelberg, Germany, **2006**, 600-601.
- (30) A. Le Bail, H. Duroy, J.L. Fourquet. *Mater. Res. Bull.* **1988**, 23, 447-452.
- 10 (31) J.M. Dance, J. Darriet, A. Tressaud, P. Hagenmüller. *Z. Anorg. Allg. Chem.* **1984**, 508, 93-99.
- (32) J.B. Goodenough. *Magnetism and the Chemical Bond*. Wiley, New York, **1963**, 75-185.
- (33) J.J. Adkin, M.A. Hayward. *J. Solid State Chem.* **2006**, 179,
- 15 70-76.
- (34) P.D. Battle, T.C. Gibb, C.W. Jones. *J. Solid State Chem.* 1988, 74, 60-66.